Available online at www.sciencedirect.com
SCIENCE DIRECT®
PERGAMON
International Journal of Heat and Mass Transfer 46 (2003) 1993–2003
International Journal of HEAT and MASS TRANSFER
www.elsevier.com/locate/ijhmt

High speed bubbly nozzle flow with heat, mass, and momentum interactions

David Albagli, Alon Gany *

Faculty of Aerospace Engineering, Technion—Israel Institute of Technology, Haifa 32000, Israel

Received 18 February 2002; received in revised form 20 October 2002

Abstract

The characteristics of high speed bubbly flows through convergent–divergent nozzles are studied theoretically. A steady, one-dimensional flow is considered. The liquid phase is water, whereas the gaseous phase consists of a mixture of both non-condensable (air) and condensable (water vapor) components. The comprehensive physical model allows for momentum and thermal lags as well as mass transfer between the gaseous and liquid phases due to evaporation and condensation. The parametric analysis reveals that choked flow with supersonic speeds along the diverging section of the nozzle, similar to the behavior of a compressible gas flow, may be obtained under appropriate conditions. Effects of flow parameters such as wall friction, interphase heat transfer, initial bubble size and void fraction are demonstrated.

1. Introduction

The behavior of bubbly mixtures flowing through convergent–divergent nozzles appears to have received little attention in the literature, and the information currently available on such flows is scarce.

One of the first studies on compressible bubbly flows was that of Tangren et al. [1], who reported a theoretical analysis and a series of experiments to validate their theory. The analysis assumed a homogeneous mixture expanding through a nozzle under absolute thermodynamic equilibrium, and the experiments were limited to pressure and thrust measurements. A similar theoretical and experimental study was reported by Mottard and Shoemaker [2], who conducted only thrust measurements. More elaborate theoretical studies were presented by Witte [3] and Amos et al. [4] on flows in which compressed air bubbles were injected into a high-pressure water stream. Their analyses abandoned the previously adopted homogeneous model in favor of the separated flow model, taking into account the fact that the two phases could have different properties (e.g., pressure and temperature) and velocities. The experimental works of Muir and Eichhorn [5] and of Thang and Davis [6] provided a rather detailed picture of air–water mixtures flowing through venturis. Their results indicated the presence of a bubbly structure at a wide flow range (up to velocities of 32 m/s and void fractions as high as 0.6).

The objective of this work is to develop a comprehensive theoretical model for bubbly nozzle flows. The model incorporates, in addition to the effects accounted for by Witte [3] and Amos et al. [4], interphase heat and mass transfer processes resulting from thermal non-equilibrium and from the presence of a condensable ingredient (water vapor) within the bubbles. The pressure loss due to wall friction, as well as surface tension and viscous effects on bubble growth, are also included in the model. The parametric study focuses on the influence of heat transfer, condensation, wall friction, bubble size, and void fraction on the development of the bubbly flow through the convergent–divergent nozzle.

* Corresponding author. Tel.: +972-4-8292554; fax: +972-4-8230956.

E-mail addresses: albagli@rafael.co.il (D. Albagli), gany@techunix.technion.ac.il (A. Gany).

0017-9310/03/$ - see front matter
doi:10.1016/S0017-9310(02)00476-3

Nomenclature

A	cross-sectional area (m^2)
a	sonic velocity ($m\,s^{-1}$)
C	coefficient
c	specific heat ($J\,kg^{-1}\,K^{-1}$)
d	flow cross-sectional diameter (m)
h	convective heat transfer coefficient ($W\,m^{-2}\,K^{-1}$)
k	thermal conductivity ($W\,m^{-1}\,K^{-1}$)
L	latent heat ($J\,kg^{-1}$)
m	mass (kg)
P	pressure ($N\,m^{-2} \equiv 10^{-5}$ bar)
R	specific gas constant ($J\,kg^{-1}\,K^{-1}$)
r	bubble radius (m)
T	temperature (K)
u	velocity ($m\,s^{-1}$)
W	molecular weight ($kg\,kg\text{-}mol^{-1}$)
x	abscissa (m)
v	kinematic viscosity ($m^2\,s^{-1}$)
ρ	density ($kg\,m^{-3}$)
σ	surface tension ($N\,m^{-1}$)
τ	wall shear stress due to friction ($N\,m^{-2}$)

Dimensionless group

f	wall friction factor ($(d/2\rho u^2)\Delta P/\Delta x$)
M	Mach number (u/a)
n	number of bubbles at a cross-section
Pr	Prandtl number ($c_p\rho v/k$)
Re	Reynolds number ($2r\Delta u/v$)
α	gas phase volume fraction
δ	mass transfer switch
μ	gas/liquid mass ratio
Φ^2	bubbly flow correction for wall friction factor
Ω	vapor volume fraction in bubble
ω	vapor mass fraction in bubble

Subscripts

D	drag
e	exit
f	friction
g	pure gas
p	constant pressure
sat	saturation
v	vapor (water)
ℓ	liquid (water)
0	nozzle entrance

Superscripts

$(\dot{})$	time derivative
$(^-)$	phase average

2. Analysis and solution procedure

2.1. Physical conditions and assumptions

The following general conditions and assumptions were used in the analysis:

- Steady, quasi-one-dimensional flow conditions prevail in the nozzle.
- The liquid and gaseous phases are in dynamic and thermal non-equilibrium.
- The flow of the liquid phase is incompressible.
- The gaseous (bubble) phase behaves like a perfect gas and has the form of finely dispersed spheres.
- The bubbles have a uniform size at any nozzle cross-section; neither coalescence nor fragmentation takes place.
- The bubbles may contain some fraction of vapor along with the non-condensable gas.
- The vapor content in the bubble is saturated during the condensation process.
- There is friction, but no heat transfer, between the flow and the nozzle walls.

2.2. Mathematical model

The mathematical model consists of the following governing equations:

2.2.1. Continuity

The two-phase continuity equation along the nozzle is

$$\dot{m}_{\mathrm{tot}} = (1+\mu_{\mathrm{o}})\rho_{\ell}u_{\ell\mathrm{o}}A_{\mathrm{o}} = [\alpha\rho u + (1-\alpha)\rho_{\ell}u_{\ell}]A \qquad (1)$$

wherein the subscript o refers to initial conditions and ℓ to the liquid (water) phase. The gaseous phase variables have no subscript. The local mass flow ratio between the gaseous and liquid phases is denoted by μ, and the volume fraction of the gaseous phase by α. The velocities of the liquid and gaseous phases are u_{ℓ} and u, respectively. A is the cross-sectional area of the nozzle and ρ is the density of the relevant phase. Note, that it is assumed that at the initial cross-section A_{o}, the two phases have equal velocities. Differentiation of Eq. (1) with respect to the variables α, ρ, u_{ℓ} and u yields:

$$\frac{dA}{dx} = -\frac{(1+\mu_o)\rho_\ell u_o A_o}{[\alpha\rho u + (1-\alpha)\rho_\ell u_\ell]^2}\left[(\rho u - \rho_\ell u_\ell)\frac{d\alpha}{dx} + \alpha u\frac{d\rho}{dx} + \alpha\rho\frac{du}{dx} + (1-\alpha)\rho_\ell\frac{du_\ell}{dx}\right] \quad (2)$$

2.2.2. Volume fraction

The volume fraction of the gaseous phase in the mixture is

$$\alpha = \frac{1}{1+\frac{\rho u}{\mu\rho_\ell u_\ell}} \quad (3)$$

Hence,

$$\frac{d\alpha}{dx} = -\frac{1}{\left(1+\frac{\rho u}{\mu\rho_\ell u_\ell}\right)^2\mu\rho_\ell u_\ell}\left(-\frac{\rho u}{\mu}\frac{d\mu}{dx} + u\frac{d\rho}{dx} + \rho\frac{du}{dx} - \frac{\rho u}{u_\ell}\frac{du_\ell}{dx}\right) \quad (4)$$

2.2.3. Momentum

$$\alpha\rho u\frac{du}{dx} + (1-\alpha)\rho_\ell u_\ell\frac{du_\ell}{dx} = -\frac{d}{dx}[\alpha P + (1-\alpha)P_\ell] - \frac{4\tau}{d} \quad (5)$$

Rearranging Eq. (5) yields:

$$\frac{dp_\ell}{dx} = -\frac{1}{1-\alpha}\left[\alpha\frac{dP}{dx} + \alpha\rho u\frac{du}{dx} + (1-\alpha)\rho_\ell u_\ell\frac{du_\ell}{dx} + (P-P_\ell)\frac{d\alpha}{dx}\right] - \frac{2\rho_\ell u_\ell^2}{d}f\Phi^2 \quad (6)$$

The last term on the RHS of both Eqs. (5) and (6) describes the effect of the friction force exerted on the fluid by the nozzle wall. The nozzle diameter is denoted by d and the wall shear stress by τ. The friction coefficient and two-phase correction factor are represented by f and Φ^2, respectively. Φ^2 may be taken as unity, since the wall friction in a turbulent bubbly flow is basically due to the liquid phase [7].

2.2.4. Bubble momentum

$$\rho u\frac{du}{dx} + \frac{1}{2}\rho_\ell\left(u\frac{du}{dx} - u_\ell\frac{du_\ell}{dx}\right) = -\frac{dP_\ell}{dx} - \frac{\frac{1}{2}C_D\rho_\ell\pi r^2|u-u_\ell|(u-u_\ell)}{\frac{4}{3}\pi r^3} - \delta\frac{u(u-u_\ell)}{\frac{4}{3}\pi r^3}\frac{1}{\dot{n}}\frac{d\dot{m}}{dx} \quad (7)$$

r is the representative bubble radius at the cross-section, C_D is the bubble drag coefficient, and $\dot{n}$ is the bubble number flow rate, which is equal to its value at the initial nozzle cross-section, i.e., $\dot{n} = \dot{n}_o = \text{const}$. The second term on the LHS of Eq. (7) is due to the additional mass effect of an accelerating bubble [8]. The last term of Eq. (7) describes the momentum change as a result of material transport from the bubble to the surroundings due to condensation or vice versa due to evaporation. The Boolean variable δ specifies whether mass transfer, (evaporation or condensation) takes place as follows:

$\delta = 0$ for $T \approx T_{sat}$: Saturation, no mass transfer.
$\delta = -1$ for $T > T_{sat}$: Evaporation of surrounding liquid.
$\delta = +1$ for $T < T_{sat}$ and $\omega > 0$: Condensation of vapor within the bubble.

Rearranging Eq. (7) yields

$$\frac{du}{dx} = -\frac{1}{(\rho + \frac{1}{2}\rho_\ell)u}\left[\frac{dP}{dx} - \frac{1}{2}\rho_\ell u_\ell\frac{du_\ell}{dx} + \frac{\frac{3}{8}C_D\rho_\ell|u-u_\ell|(u-u_\ell)}{r} + \delta\frac{(u-u_\ell)}{\frac{4}{3}\pi r^3}\frac{1}{\dot{n}}\frac{d\dot{m}}{dx}\right] \quad (8)$$

2.2.5. Bubble thermal energy

$$4\pi r^2 h(T_\ell - T) = (1-|\delta|)\frac{4}{3}\pi r^3\rho c_p u\frac{dT}{dx} + \delta L_v u\frac{1}{\dot{n}}\frac{d\dot{m}}{dx} \quad (9)$$

The LHS of Eq. (9) describes the heat absorbed by the bubble under forced convection, where h is the heat transfer coefficient, c_p is the bubble specific heat and L_v is the latent heat of evaporation of the liquid phase.

Using the ideal gas relationship

$$P = \rho RT \quad (10)$$

and Eq. (9), one obtains

$$\frac{dP}{dx} = \frac{3Rh(T_\ell - T)}{rc_p u} - \frac{3P}{r}\frac{dr}{dx} \quad \text{for } \delta = 0 \quad (11)$$

$$\frac{dr}{dx} = \frac{h(T_\ell - T)}{\rho u L_v} + \frac{r}{3R}\frac{dR}{dx} - \frac{r}{3P}\frac{dP}{dx} + \frac{r}{3T}\frac{dT}{dx} \quad \text{for } |\delta| = 1 \quad (12)$$

In Eqs. (11) and (12) it was assumed that the pressure within the bubble is practically equal to the local liquid pressure during the condensation process. This assumption was found to be fully justified for the size of bubbles relevant to this study.

2.2.6. Bubble radius

The displacement of the bubble wall in the absence of interphase mass transfer was first analyzed by Rayleigh [9]. Additional effects of interphase slip, viscosity and

surface tension were suggested by Knapp et al. [10], yielding the following equation:

$$\frac{P-P_\ell}{\rho_\ell} = ru^2\frac{\mathrm{d}^2 r}{\mathrm{d}x^2} + \frac{3}{2}\left(u\frac{\mathrm{d}r}{\mathrm{d}x}\right)^2 - \frac{(u-u_\ell)^2}{4} + \frac{4v_\ell u}{r}\frac{\mathrm{d}r}{\mathrm{d}x} + \frac{2\sigma_\ell}{\rho_\ell r} \quad \text{for } \delta = 0 \tag{13}$$

Hence,

$$\frac{\mathrm{d}^2 r}{\mathrm{d}x^2} = \frac{P-P_\ell}{\rho_\ell r u^2} - \frac{1}{u}\frac{\mathrm{d}u}{\mathrm{d}x}\frac{\mathrm{d}r}{\mathrm{d}x} - \frac{3}{2r}\left(\frac{\mathrm{d}r}{\mathrm{d}x}\right)^2 + \frac{(u-u_\ell)^2}{4ru^2} - \frac{4v_\ell}{r^2 u}\frac{\mathrm{d}r}{\mathrm{d}x} - \frac{2\sigma_\ell}{\rho_\ell r^2 u^2} \quad \text{for } \delta = 0 \tag{14}$$

When condensation or evaporation takes place, Eq. (12) rather than Eq. (14) is used in order to describe the bubble radius change.

2.2.7. Mass flow rate ratio

The local value of the bubble to liquid mass flow rate ratio is:

$$\mu = \frac{\dot{m}}{\dot{m}_\ell} \tag{15}$$

where $\dot{m}$ and $\dot{m}_\ell$ are the local mass flow rates of gaseous and liquid phases, respectively. Differentiation of Eq. (15) yields:

$$\frac{\mathrm{d}\mu}{\mathrm{d}x} = \delta\frac{1}{(1+\mu)\dot{m}_\ell}\frac{\mathrm{d}\dot{m}}{\mathrm{d}x} = \delta\frac{(1+\mu)^2}{(1+\mu_\mathrm{o})\dot{m}_{\ell\mathrm{o}}}\frac{\mathrm{d}\dot{m}}{\mathrm{d}x} \tag{16}$$

Note that in the absence of mass transfer between the liquid and gaseous phases ($\delta = 0$), the local mass flow rate ratio remains constant ($\mathrm{d}\mu/\mathrm{d}x = 0$).

The interphase mass transfer rate can be evaluated by the relation:

$$\frac{\mathrm{d}\dot{m}}{\mathrm{d}x} = -\frac{\mathrm{d}\dot{m}_\ell}{\mathrm{d}x} = \delta\frac{4\pi r^2 \dot{n} h(T_\ell - T)}{uL_\mathrm{v}} \tag{17}$$

2.2.8. Bubble humidity

The vapor mass fraction within the bubble is defined as follows:

$$\omega = \frac{m_\mathrm{v}}{m_\mathrm{g}+m_\mathrm{v}} = \frac{\dot{m}_\mathrm{v}}{\dot{m}_\mathrm{g}+\dot{m}_\mathrm{v}} \tag{18}$$

where the indices g and v stand for the gas (non-condensable) and vapor (condensable) ingredients within the bubble, respectively. The vapor volume fraction Ω within the bubble can be related to its mass fraction ω:

$$\Omega = \frac{\omega}{\omega + (1-\omega)W_\mathrm{v}/W_\mathrm{g}} \tag{19}$$

where W stands for molecular weight.

Taking into account that the mass of the non-condensable gas within the bubble remains constant, one obtains:

$$\frac{\mathrm{d}\omega}{\mathrm{d}x} = \frac{\dot{m}_\mathrm{g}}{\dot{m}^2}\frac{\mathrm{d}\dot{m}}{\mathrm{d}x} = \frac{(1-\omega)}{\frac{4}{3}\pi r^3 \rho}\frac{1}{\dot{n}}\frac{\mathrm{d}\dot{m}}{\mathrm{d}x} \tag{20}$$

The mass transfer rate between the bubbles and the surrounding can be expressed explicitly as:

$$\frac{\mathrm{d}\dot{m}}{\mathrm{d}x} = \delta 4\pi r^2 \dot{n}\rho_\mathrm{v}\frac{\mathrm{d}r}{\mathrm{d}x} = \delta 4\pi r^2 \dot{n}\rho\frac{W_\mathrm{v}}{W}\frac{\mathrm{d}r}{\mathrm{d}x} \tag{21}$$

yielding

$$\frac{\mathrm{d}\omega}{\mathrm{d}x} = \delta\frac{3(1-\omega)}{r}\frac{W_\mathrm{v}}{W}\frac{\mathrm{d}r}{\mathrm{d}x} \tag{22}$$

where W and ρ are the mean molecular weight and density of the bubble content, respectively. The mean molecular weight is calculated from:

$$W = \frac{1}{\frac{\omega}{W_\mathrm{v}} + \frac{1-\omega}{W_\mathrm{g}}} \tag{23}$$

2.2.9. Other flow properties and auxiliary relations

One of the main flow characteristics is the flow Mach number M, defined as the mean mixture velocity $\overline{u}$ divided by the speed of sound a:

$$M = \frac{\overline{u}}{a} \tag{24}$$

The mean velocity is taken as the mixture's center of mass velocity:

$$\overline{u} = \frac{\alpha\rho u + (1-\alpha)\rho_\ell u_\ell}{\alpha\rho + (1-\alpha)\rho_\ell} \tag{25}$$

The speed of sound, which is the propagation velocity of infinitesimal pressure perturbations in thermal equilibrium, is given by the following expression for bubbly flows [2,11]:

$$a = \left(\frac{\mathrm{d}P}{\mathrm{d}\rho}\right)_T^{1/2} = \left(1+\frac{\rho}{\mu\rho_\ell}\right)\left(\mu\frac{P}{\rho}\right)^{1/2} \tag{26}$$

Interestingly, the typical value of the speed of sound in bubbly mixtures is lower by one to two orders of magnitude than that of either the gas or liquid phases alone. Fig. 1 shows, for example, the speed of sound in water–air mixtures vs. the air/water mass ratio μ, revealing that the presence of a small fraction of either phase in the other is enough to cause a substantial reduction in sonic velocity.

As is shown in Eqs. (7) and (8), the bubble motion is affected by its drag coefficient C_D, which may be represented by the following correlations [12]:

$$C_\mathrm{D} = \frac{24}{Re}\left(1+\frac{3}{16}Re\right) \quad Re \leqslant 1 \tag{27a}$$

$$C_\mathrm{D} = 10^{(1.455-0.912\log_{10} Re)} \quad 1 < Re \leqslant 4 \tag{27b}$$

$$C_\mathrm{D} = \frac{18.5}{Re^{0.6}} \quad 4 < Re \leqslant 500 \tag{27c}$$

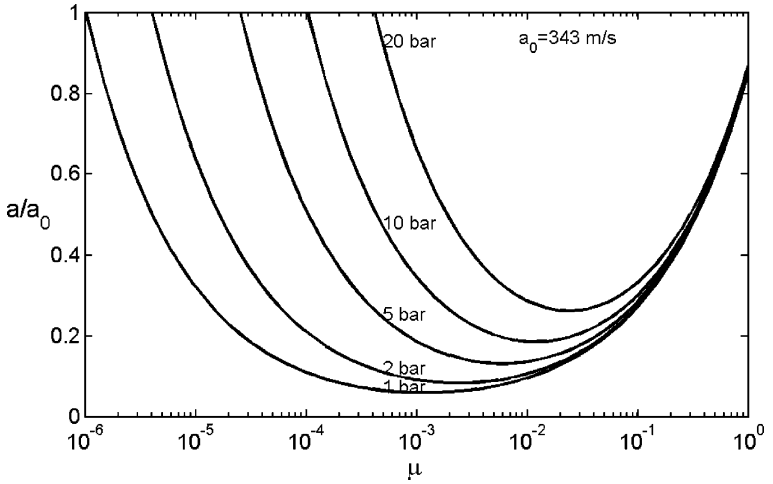

Fig. 1. Speed of sound in water–air mixtures vs. air/water mass ratio.

$$C_D = 0.444 \quad 500 < Re \tag{27d}$$

In Eqs. (27a)–(27d), Reynolds number of the bubble is defined as:

$$Re = \frac{2r|u - u_\ell|}{v_\ell} \tag{28}$$

The asymptotic value of the friction factor f at smooth internal walls for high Reynolds numbers is taken from Moody [13]:

$$f = 0.0063 \tag{29}$$

A correlation for the heat transfer coefficient h between the bubble and the surrounding liquid (see Eqs. (9), (11), (12) and (17)) is given by Vliet and Leppert [14]:

$$h = \frac{k_\ell}{2r}(1.3Pr^{0.15} + 0.66Pr^{0.31}Re^{0.5}) \tag{30}$$

where Prandtl number Pr is defined as:

$$Pr = \frac{\rho_\ell v_\ell c_{p\ell}}{k_\ell} \tag{31}$$

The saturation temperature of the vapor is related to its partial pressure within the bubble according to Clausius–Clapeyron equation:

$$\frac{dP_v}{P_v} = \frac{L_v}{R_v}\frac{dT}{T^2} \tag{32}$$

Note that the vapor pressure is a function of pressure within the bubble as follows:

$$P_v = \frac{\omega}{\omega + (1-\omega)W_v/W_g}P \tag{33}$$

2.2.10. Solution technique

Following the development of the physical model in the previous section, a system of nine non-linear, first order, ordinary differential equations can be formed. Each of these equations is a function of a series of variables:

$$\frac{d^2r}{dx^2} = \varphi_1\left(\frac{dr}{dx}, \frac{du}{dx}, r, P, P_\ell, u, u_\ell\right) \tag{34}$$

$$\frac{dr}{dx} = \varphi_2\left(\frac{d^2r}{dx^2}, r, \omega, T, P, u\right) \tag{35}$$

$$\frac{d\mu}{dx} = \varphi_3(r, \mu, T, u) \tag{36}$$

$$\frac{dw}{dx} = \varphi_4\left(\frac{dr}{dx}, r, \omega, T, P\right) \tag{37}$$

$$\frac{dT}{dx} = \varphi_5(r, \omega, T, u, P) \tag{38}$$

$$\frac{dP}{dx} = \varphi_6\left(\frac{dr}{dx}, \frac{d\omega}{dx}, \frac{dT}{dx}, r, T, P, u\right) \tag{39}$$

$$\frac{du}{dx} = \varphi_7\left(\frac{dr}{dx}, \frac{dP}{dx}, \frac{du_\ell}{dx}, r, \omega, T, P, u, u_\ell\right) \tag{40}$$

$$\frac{dP_\ell}{dx} = \varphi_8\left(\frac{d\mu}{dx}, \frac{d\omega}{dx}, \frac{dT}{dx}, \frac{dP}{dx}, \frac{du}{dx}, \frac{du_\ell}{dx}, \mu, \omega, T, P, P_\ell, u, u_\ell\right) \tag{41}$$

$$\frac{du_\ell}{dx} = \varphi_9\left(\frac{dA}{dx}, \frac{d\mu}{dx}, \frac{d\omega}{dx}, \frac{dT}{dx}, \frac{dP}{dx}, \frac{du}{dx}, \frac{du_\ell}{dx}, r, \mu, \omega, T, P, P_\ell, u, u_\ell\right) \tag{42}$$

The system consists of nine dependent variables: r, μ, ω, T, P, P_ℓ, u, u_ℓ, and A. Other variables such as $\dot{m}$, α, δ and Ω can be calculated from algebraic expressions.

The strong coupling and high non-linearity of the equations do not permit analytical solutions. Rather, a numerical solution is sought.

The solution in the present work was obtained by Gear's numerical method [15]. Note that one of the nine variables mentioned above should be kept as a free variable, since both of the first two equations, (34) and (35), result from the second order equation for the bubble radius (Eq. (14)). In principle, one can prescribe a distribution for any one of the variables and solve for the rest. However, when specifying the free variable distribution one should be aware of the physical constraints, e.g., not to exceed a certain bubble volume fraction in order to maintain a bubbly flow regime.

In addition to the free variable distribution along the nozzle, boundary conditions for all variables at the nozzle inlet section have to be given.

3. Results and discussion

The bubbly flow analysis was used to solve two-phase nozzle flows of water–gas (mainly air) mixtures. Representative calculations were made for a set of fixed properties, where a number of key parameters were systematically varied, revealing the effects of these parameters on the flow characteristics. The following properties at the nozzle initial cross-section were kept constant in all cases investigated:

nozzle inlet diameter	$d_o = 0.079$ m
static pressure	$P_o = 1$ MPa
flow velocity	$u_o = u_{\ell o} = 25$ m/s
bubble radius	$r_o = 0.001$ m
bubble volume fraction	$\alpha_o = 0.20$
water temperature	$T_\ell = 293$ K
bubble temperature	$T_o \cong 480$ K (adiabatic compression from 0.1 to 1 MPa)

When the effect of condensable gas on the bubbly flow was studied, the bubbles contained initial fractions of 50% water vapor and 50% non-condensable gas by volume (i.e., $\Omega_o = 0.5$), implying an initial equilibrium bubble temperature of $T_o \cong 420$ K.

In addition to the constant values at the initial cross-section, the flow velocity gradient was kept fixed at the value of $du/dx = 100\ s^{-1}$ throughout the nozzle length.

The nozzle exit was defined as the cross-section where the flow static pressure dropped to the value of the ambient pressure, 0.1 MPa.

3.1. General flow characteristics with non-condensable gases

Schematic of the nozzle configuration and the corresponding flow notation is given in Fig. 2.

Fig. 3 presents the variations of major properties along the nozzle for water flow with air bubbles, neglecting the effect of condensable (vapor) component. The value of the local nozzle diameter results from the requirement of constant du/dx, and from the corresponding pressure gradient. Interestingly, these conditions yield a supersonic exit velocity $\overline{u}_e$ (Mach number M_e of the order of 2.5), while the nozzle gets a convergent–divergent shape. This behavior is similar to that of compressible gas flows and results from the compressibility of the bubbles. Note, however, at atmospheric pressure the sonic velocity in the bubbly flow is remarkably low, of the order of 25 m/s, for void fractions relevant to our study (see Fig. 1). In addition, since the flow expansion is only due to the gas (bubble) phase, the final flow velocity $\overline{u}_e$ cannot largely exceed the value of water velocity corresponding to a complete conversion of the initial water stagnation pressure to dynamic pressure.

Pressure gradient, which appears to be almost constant along the nozzle, causes the bubble velocity to always exceed the water velocity after the initial cross-section. For the bubble size and flow characteristics investigated, the difference between the internal bubble pressure and the surrounding flow pressure was found negligible.

Similar to any compressible nozzle flow, the accelerating two-phase mixture may reach sonic velocity at the narrowest cross-section (throat). For further ac-

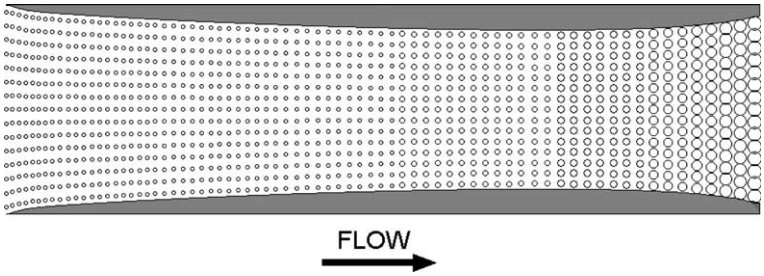

Fig. 2. Definition sketch for nozzle flow, indicating bubble size evolution.

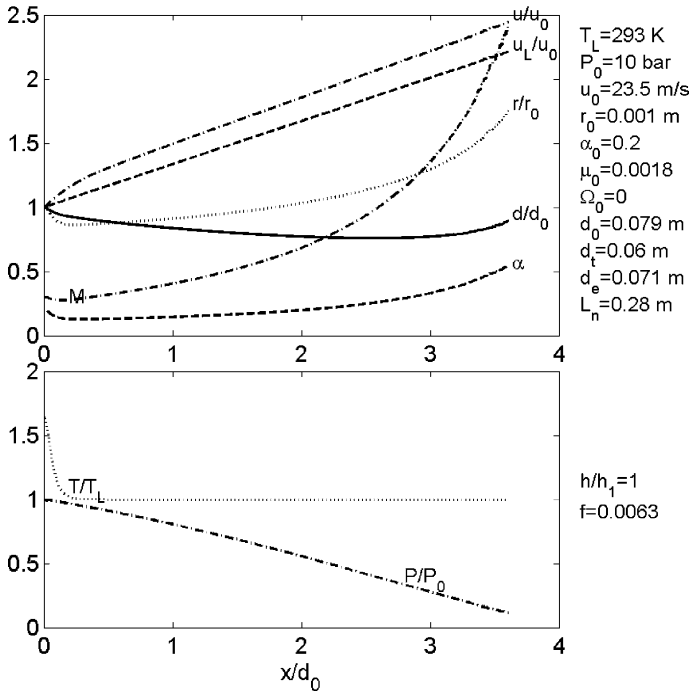

Fig. 3. Development of flow along the nozzle (pure air bubbles injected at an initial temperature of 480 K).

celeration of the mixture, the nozzle must have a divergent section with a negative downstream pressure gradient.

Bubble temperature is shown to drop fairly rapidly (typically it reaches the water temperature within less than 10% of the nozzle length in this configuration). This temperature drop results in a pronounced reduction in the bubble radius and in the bubble phase volume fraction during the initial part of the nozzle. Further downstream, however, the consistently decreasing pressure causes a monotonic increase in the bubble radius as well as in the bubble phase volume fraction after the initial dip.

Calculations conducted for the same conditions, using gaseous hydrogen (instead of air) bubbles showed that, when keeping identical bubble size and gas phase volume fraction, there is practically no difference in the development of the flow. This behavior results from the fact that the most relevant gas phase properties, such as the response to pressure and temperature variations as well as the overall heat capacity (sensible enthalpy), are proportional to the number of moles, represented by the gas volume. Some deviation from this behavior may occur when using gases of different molecular structure, e.g., monatomic (He) or triatomic (CO_2) vs. the diatomic gases investigated. A good similarity criterion is the value of the specific heats ratio, γ.

3.2. Friction effects

Friction losses at the nozzle walls have some effect on the flow development. The most significant result may be the influence on the exit flow velocity and Mach number. Fig. 4 shows the variation of exit velocity with the friction coefficient for the same nozzle inlet and exit pressures. The standard friction coefficient for large Reynolds numbers ($f_1 = 0.0063$) was taken from Moody [13]. The exit velocity and Mach number were found to decrease when increasing the friction coefficient and vice versa. Of course, the highest exit velocity and Mach number values correspond to frictionless conditions. In addition, under the condition of constant du/dx, the nozzle length is directly proportional to the exit velocity.

It should be noted that, although the absolute values of the exit velocity seem to vary only slightly with the friction coefficient, the effect is quite significant and may result in a complete loss of the energy (and potential momentum) added to the flow by the compressed gas.

3.3. Condensable ingredient effect

Bubbles containing a condensable ingredient (water vapor) undergo mass transfer interactions with the surrounding water in addition to heat transfer, as a result of condensation/evaporation processes during the expansion in the nozzle.

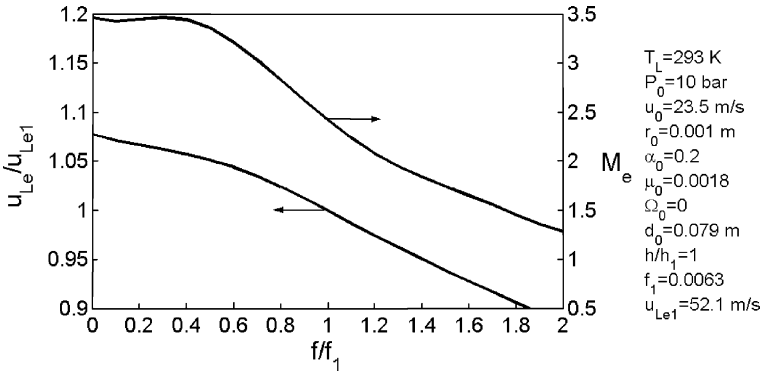

Fig. 4. Effect of friction factor f on nozzle exit velocity $u_{\ell e}$ and Mach number M_e (f_1 refers to nominal case).

Fig. 5 shows the development of the flow along the nozzle for bubbles consisting of 50% air and 50% water vapor by volume, accounting for the phase change effects. Condensation progresses along the liquid–vapor saturation line (Eq. (32)), dictated from the interfacial heat exchange and local pressure.

Condensation causes some reduction in the exit flow Mach number and velocity compared to the case of non-condensable bubbles, when using the same initial overall bubble phase volume fraction. The reason for this behavior is that during condensation part of the bubble mass is converted into liquid, hence the local volume fraction as well as the expansion capacity of the bubbles decrease.

The condensation process is significantly affected by the interfacial heat transfer. A decrease in the heat loss rate from the bubble to the surrounding water, as may occur in the presence of a non-condensable gas or certain contaminants at the bubble–water interface, slows down the condensation rate. The heat transfer effect was

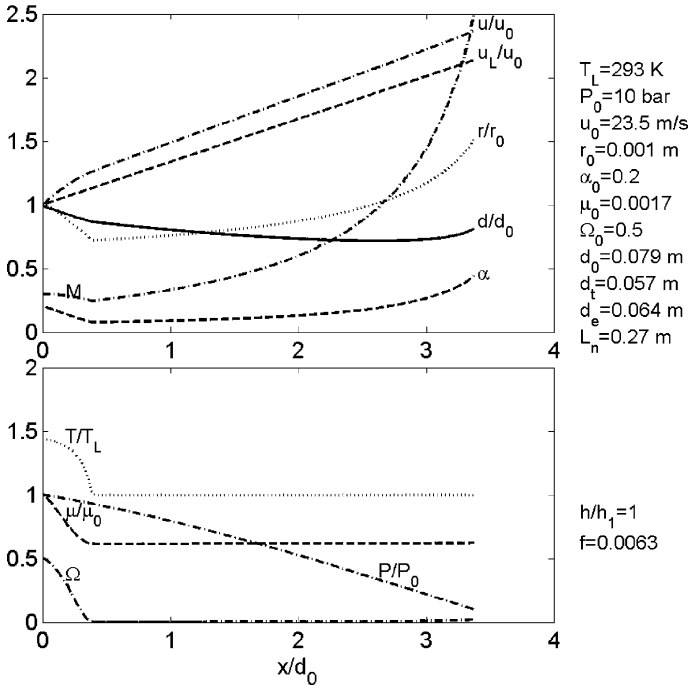

Fig. 5. Development of flow along the nozzle, accounting for phase change effect (bubbles containing air + vapor injected at an initial temperature of 420 K).

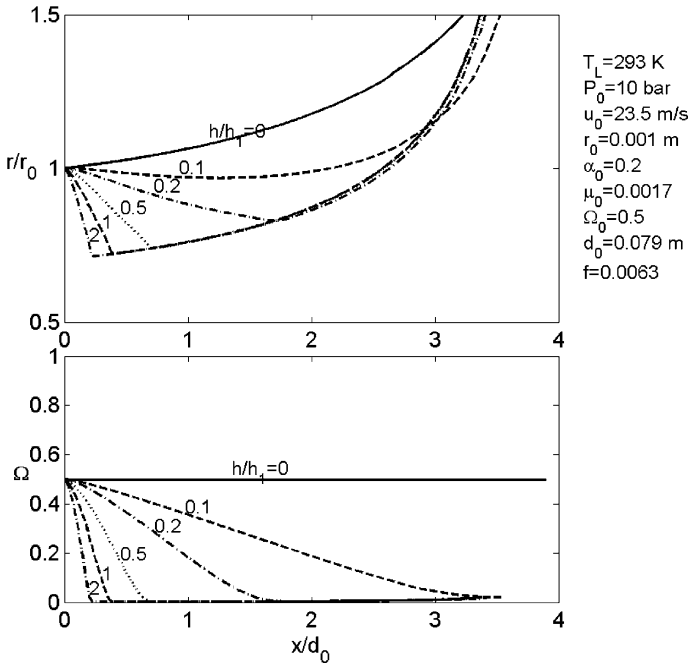

Fig. 6. Effect of heat transfer coefficient h on: (a) vapor volume fraction Ω in the bubble, (b) bubble radius r (h_1 refers to nominal case).

studied parametrically by using different theoretical values of the convection heat transfer coefficient h. The results are presented in Fig. 6.

Although the effect of heat transfer on the condensation process and on the bubble size variations is pronounced, the overall influence on the final flow velocity is almost negligible as long as the condensation process ends within the nozzle. Noticeable effects on the exit flow conditions are predicted only if part of the vapor in the bubbles remains uncondensed throughout the entire nozzle length. Theoretically, this requires heat transfer coefficients as low as 10% of the nominal value h_1.

It should be mentioned again that, when dealing with the same volume fractions of the water vapor and the non-condensable gas within the bubble, there is virtually no effect of the type of the non-condensable gas on the entire process.

3.4. Other effects

Bubble size affects the flow development particularly through heat transfer. The larger the bubbles, the lower the cooling and condensation rates, resulting in longer condensation distances (Fig. 7). However, for the bubble

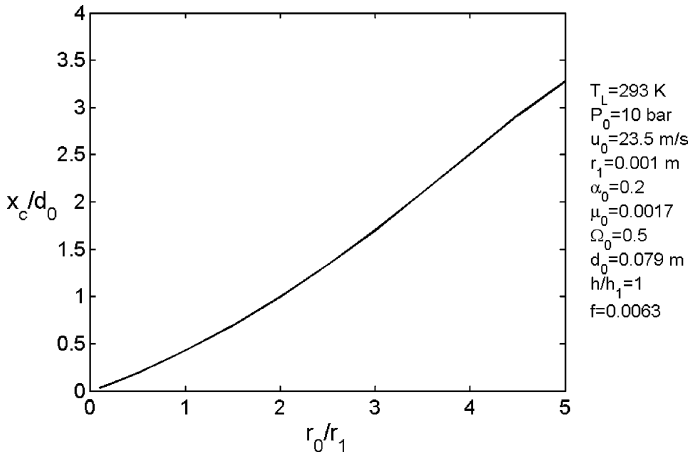

Fig. 7. Effect of initial bubble radius r_o on condensation distance x_c (r_1 refers to nominal case).

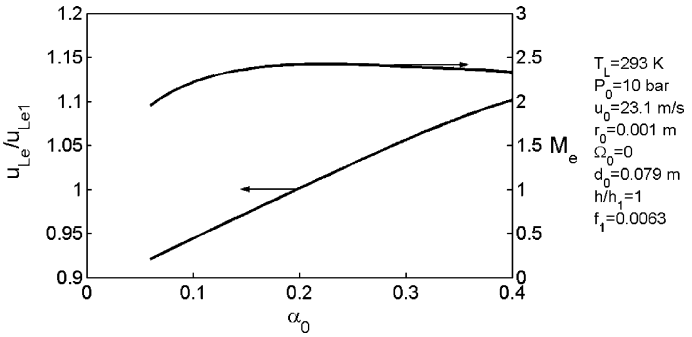

Fig. 8. Effect of initial void fraction α_o on nozzle exit velocity $u_{\ell e}$ and Mach number M_e.

size and nozzle dimensions concerned, thermal equilibrium between the bubbles and the surrounding water is achieved at the initial part of the nozzle. Hence, the overall effect on the final flow conditions seems to be minor.

The thermal behavior of the bubbles indicate that the initial bubble temperature plays only a minor role in the flow development process, unless the heat transfer rate is very low. Typically, the bubbles lose their sensible enthalpy very rapidly, thereby reducing the volume fraction by approximately the ratio between the initial water and gas absolute temperatures. The overall impact on the flow is almost equal to that of a cold gas at a lower volume fraction. In this respect, the gas–water mass ratio, rather than the volume ratio, should be used for comparing bubbly flows of the same gas at different initial temperatures.

Investigating the void fraction effect, one finds that although the exit Mach number has a maximum around $\alpha_o = 0.2$, the exit velocity tends to increase with increasing the initial void fraction (Fig. 8). This trend is less pronounced for α_o values over 0.4. It should be noted that such initial void fractions imply final gas volume fractions as high as 0.7, indicating uncertainties as to whether bubbly flow regime could be maintained. It is noted that the geometric limit of gas volume fraction in a uniform bubbly flow is $\pi/\sqrt{18} \cong 0.74$, corresponding to face centered cubic lattice configuration or "orange-pile" packing [16].

4. Concluding remarks

Choking conditions with supersonic exit velocity can be achieved for bubbly mixtures flowing through convergent–divergent nozzles. The gas energy added by injecting the bubbles to the water flow may accelerate the flow to exit velocities higher than those corresponding to a complete conversion of the initial water stagnation pressure to dynamic pressure (kinetic energy). However, wall friction may cause a significant decrease in the actual energy (and velocity) contribution to the flow. Thermal energy, expressed by a high initial bubble temperature, is often totally useless regarding its conversion to kinetic energy and its contribution to the flow velocity. This behavior results from the rapid cooling of the bubbles. Condensable ingredient (water vapor) in the bubble in the account of a non-condensable gas is expected to be almost as ineffective as a high sensible enthalpy (temperature) due to the condensation process whose characteristic time is shorter than that of the residence time in the nozzle. The effect of condensable gas may increase at shorter nozzles and for reduced heat transfer coefficients.

References

[1] R.F. Tangren, C.H. Dodge, H.S. Seifert, Compressibility effects in two-phase flow, J. Appl. Phys. 20 (1949) 637–645.
[2] E.J. Mottard, C.J. Shoemaker, Preliminary Investigation of an Underwater Ramjet Powered by Compressed Air, NASA Rept. TND-991, Washington, DC, 1961.
[3] J.H. Witte, Predicted performance of large water Ramjets, in: AIAA 2nd Advanced Marine Vehicles and Propulsion Meeting, Seattle, WA, 1969, AIAA Paper 69-406.
[4] R.G. Amos, G. Maples, D.F. Dyer, Thrust of an air-augmented waterjet, J. Hydronaut. 7 (1973) 64–71.
[5] J.H. Muir, R. Eichhorn, Compressible flow of an air–water mixture through a vertical, two-dimensional, converging–diverging nozzle, in: Proceedings of the 1963 Heat Transfer and Fluid Mechanics Institute, Stanford, CT, 1963, pp. 183–204.
[6] N.T. Thang, M.R. Davis, The structure of bubbly flow through venturis, Int. J. Multiphase Flow 5 (1979) 17–37.
[7] G.B. Wallis, in: One-Dimensional Two-Phase Flow, McGraw-Hill, New York, 1969, p. 28.
[8] S.L. Soo, in: Fluid Dynamics of Multiphase Systems, Blaisdell, New York, 1967, pp. 31–43.
[9] Lord Rayleigh, On the pressure developed in a liquid during the collapse of a spherical cavity, Philos. Mag. 34 (1917) 94–98.
[10] R.T. Knapp, J.W. Daily, F.G. Hammitt, in: Cavitation, McGraw-Hill, New York, 1970, pp. 104–131.

[11] R.E. Henry, M.A. Grolmes, H.K. Fauske, Propagation velocity of pressure waves in gas–liquid mixtures, in: Cocurrent Gas–Liquid Flow, Plenum, New York, 1969, pp. 1–18.
[12] H. Schlichting, in: Boundary Layer Theory, McGraw-Hill, New York, 1968, p. 17.
[13] L.F. Moody, Friction factors for pipe flow, Trans. ASME 66 (1944) 671–684.
[14] G.C. Vliet, G. Leppert, Forced convection heat transfer from an isothermal sphere to water, J. Heat Transfer 83 (1961) 163–175.
[15] C.W. Gear, in: Numerical Initial Value Problems in Ordinary Differential Equations, Prentice-Hall, New Jersey, 1971, pp. 209–228.
[16] K.J. Devlin, Mathematics—The Science of Patterns, Scientific American Library, New York, 1994, p. 157.